molecular pharmaceutics

articles

HPMA Copolymer-Bound Doxorubicin Induces Apoptosis in Ovarian Carcinoma Cells by the Disruption of Mitochondrial Function

Alexander Malugin,[†] Pavla Kopečková,[†,‡] and Jindřich Kopeček*[,†,‡]

Department of Pharmaceutics and Pharmaceutical Chemistry and Department of Bioengineering, University of Utah, Salt Lake City, Utah 84112

Received August 22, 2005

Abstract: *N*-(2-Hydroxypropyl)methacrylamide (HPMA) copolymer-bound doxorubicin has showed greater potency than free doxorubicin in the treatment of ovarian cancer in vivo and in vitro. The promising activity of the conjugate demonstrated in clinical trials has generated considerable interest in understanding the mechanism of action of this macromolecular therapeutic. In this study, the involvement of the mitochondrial pathway in HPMA copolymer-bound doxorubicin-induced apoptosis in the human ovarian cancer cell line A2780 was investigated. Through a series of in vitro assays, including confocal microscopy, flow cytometry, and spectrofluorimetry, a significant decrease in mitochondrial membrane potential in A2780 cells treated with HPMA copolymer-bound doxorubicin was found. The most dramatic changes in mitochondrial membrane potential were observed between 2 and 12 h of continuous drug exposure. The potential of the mitochondrial membrane remained collapsed when drug treatment continued up to 24 h. For the first time, it was shown that HPMA copolymer-bound doxorubicin induces apoptosis in ovarian cancer cells by simultaneous activation of both caspase-dependent and caspase-independent pathways of DNA damage. This was determined by monitoring the translocation of the mitochondrial proteins cytochrome *c* and apoptosis-inducing factor to cytosol. The altered balance between anti-apoptotic and pro-apoptotic members of the Bcl-2 family of proteins was responsible for the mitochondrial function distraction. HPMA copolymer-bound doxorubicin induced a time-dependent decrease in the expression of the anti-apoptotic Bcl-2 and Bcl-x_L proteins, which control cell survival. At the same time, the expression level of pro-apoptotic members (Bax, Bad) of the Bcl-2 family was increased under the chosen experimental conditions. Altogether, these results indicate that HPMA copolymer-bound doxorubicin induced apoptosis in ovarian cancer cells through the mitochondrial pathway.

Keywords: Anticancer agents; apoptosis; cell culture; HPMA copolymer; doxorubicin; mitochondria; macromolecular therapeutics

Introduction

Since the discovery of its fundamental role in the regulation of tissue development and homeostasis through cell death,[1] the stimulation of "apoptotic machinery"[2] remains an attractive strategy for cancer treatment. An increasing line of evidence indicates that the molecular components essential for apoptosis induction are present in all cells, and only

* To whom correspondence should be addressed. Mailing address: Department of Pharmaceutics and Pharmaceutical Chemistry, University of Utah, 30 S., 2000 E., Rm. 201, Salt Lake City, UT 84112. Phone: (801) 581-7211. Fax: (801) 581-7848. E-mail: Jindrich.Kopecek@m.cc.utah.edu.

† Department of Pharmaceutics and Pharmaceutical Chemistry.

‡ Department of Bioengineering.

(1) Kerr, J. F.; Wyllie, A. H.; Currie, A. R. Apoptosis: A Basic Biological Phenomenon with Wide-Ranging Implications in Tissue Kinetics. *Br. J. Cancer* **1972**, *26*, 239−257.

(2) Ghobrial, I. M.; Witzig, T. E.; Adjei, A. A. Targeting Apoptosis Pathways in Cancer Therapy. *CA Cancer J. Clin.* **2005**, *55*, 178−194.

10.1021/mp050065e CCC: $33.50
Published on Web 03/23/2006

require the proper trigger.[3] Apoptosis can be initiated though multiple death receptors[4] located on the plasma membrane, or it can begin through intracellular events and pathways.[5] Regardless of how initiated, apoptotic processes typically end with the activation of cysteine proteases that cleave at aspartate residues (caspases), which are considered to be major executioners of initiated cell death.[6] The exact molecular mechanism of apoptosis is not completely clear, but it appears that a variety of key events are focused on mitochondria.[7] Alteration of mitochondrial respiration, changes in electron transport, production of reactive oxygen species, loss of mitochondrial membrane potential, induction of the mitochondrial permeability transition, and release of caspase activators are among these events.[3−5,7,8]

The idea about the unique role of mitochondria, not only as an energy producing organelle, but also as a central regulator of cell death, was not easily accepted until the pioneering work of G. Kroemer. His team discovered that alteration of mitochondrial membrane permeabilization played a pivotal role in early steps of the apoptotic process.[9] Later, X. Wang and colleagues found that cytochrome *c*, an important component of mitochondrial electron chain transfer, is a caspase activator.[10] In cytosol, cytochrome *c* triggers the activation of a caspase cascade. Active caspases ultimately trigger the caspase-dependent DNase (CAD) in the nucleus. CAD, in turn, induces oligonucleosomal DNA degradation.[11] There are many other proteins that can be released from mitochondria upon the stimulation of apoptosis.[12,13] Apoptosis-inducing factor (AIF), for example, is released from mitochondria, translocates to the nucleus,[14] and interacts with DNA and the latent DNase cyclophilin A.[15] This interaction results in DNA fragmentation and nuclear condensation.[16] In contrast to cytochrome *c*, AIF-induced DNA fragmentation is caspase-independent.[17] However, despite this evidence, candidates other than mitochondria were promoted for the central role in apoptotic cell death.[18,19]

The Bcl-2 family proteins represent another class of key regulators of cell death and survival. Based on their homology to Bcl-2 and their function, members of the Bcl-2 family are divided into an anti-apoptotic group, or the Bcl-2 subfamily (Bcl-2, Bcl-xL, Mcl-1, Bcl-w, and A1/Bfl-1), and a pro-apoptotic group, including the Bax subfamily (Bax, Bak, Bok/Mtd) and the BH3 subfamily (Bik, Hrk/DP5, BimL, Bad, Noxa, Puma, Bmf, and Bid).[20] Anti-apoptotic Bcl-2 family members function by well-orchestrated interactions with pro-apoptotic family members.[21] Pro-apoptotic Bcl-2 family members, in response to apoptotic stimuli, can form heterodimers with anti-apoptotic members located in the outer mitochondrial membrane, and regulate membrane permeability.[20] Recent studies have shown that therapeutic agents may target proteins of the Bcl-2 family, affect mitochondrial outer membrane permeabilization, and initiate an apoptotic cell death.[22]

(3) Debatin, K. M.; Krammer P. H. Death Receptors in Chemotherapy and Cancer. *Oncogene* **2004**, *23*, 2950−2966.

(4) Kim, R. Recent Advances in Understanding the Cell Death Pathways Activated by Anticancer Therapy. *Cancer* **2005**, *103*, 1551−1560.

(5) Adams, J. M. Ways of Dying: Multiple Pathways to Apoptosis. *Genes Dev.* **2003**, *17*, 2481−2489.

(6) Earnshaw, W. C.; Martins, L. M.; Kaufmann, S. H. Mammalian Caspases: Structure, Activation, Substrates, and Functions During Apoptosis. *Annu. Rev. Biochem.* **1999**, *68*, 383−424.

(7) Kroemer, G.; Reed, J. C. Mitochondrial Control of Cell Death. *Nat. Med.* **2000**, *6*, 513−519.

(8) Debatin, K. M.; Poncet, D.; Kroemer, G. Chemotherapy: Targeting the Mitochondrial Cell Death Pathway. *Oncogene* **2002**, *21*, 8786−8803.

(9) Kroemer, G.; Petit, P.; Zamzami, N.; Vayssiere, J. L.; Mignotte, B. The Biochemistry of Programmed Cell Death. *FASEB J.* **1995**, *9*, 1277−1287.

(10) Liu, X.; Kim, C. N.; Yang, J.; Jemmerson, R.; Wang, X. Induction of Apoptotic Program in Cell-Free Extracts: Requirement for dATP and Cytochrome *c*. *Cell* **1996**, *86*, 147−157.

(11) Nagata, S. DNA Degradation in Development and Programmed Cell Death. *Annu. Rev. Immunol.* **2005**, *23*, 853−875.

(12) Patterson, S. D.; Spahr, C. S.; Daugas, E.; Susin, S. A.; Irinopoulou, T.; Koehler, C.; Kroemer, G. Mass Spectrometric Identification of Proteins Released from Mitochondria Undergoing Permeability Transition. *Cell Death Differ.* **2000**, *7*, 137−144.

(13) van Loo, G.; Schotte, P.; van Gurp, M.; Demol, H.; Hoorelbeke, B.; Gevaert, K.; Rodriguez, I.; Ruiz-Carrillo, A.; Vandekerckhove, J.; Declercq, W.; Beyaert, R.; Vandenabeele, P. Endonuclease G: A Mitochondrial Protein Released in Apoptosis and Involved in Caspase-Independent DNA Degradation. *Cell Death Differ.* **2001**, *8*, 1136−1142.

(14) Daugas, E.; Susin, S. A.; Zamzami, N.; Ferri, K. F.; Irinopoulou, T.; Larochette, N.; Prevost, M. C.; Leber, B.; Andrews, D.; Penninger, J.; Kroemer, G. Mitochondrio-Nuclear Translocation of AIF in Apoptosis and Necrosis. *FASEB J.* **2000**, *14*, 729−739.

(15) Cande, C.; Vahsen, N.; Kouranti, I.; Schmitt, E.; Daugas, E.; Spahr, C.; Luban, J.; Kroemer, R. T.; Giordanetto, F.; Garrido, C.; Penninger, J. M.; Kroemer, G. AIF and Cyclophilin A Cooperate in Apoptosis-Associated Chromatinolysis. *Oncogene* **2004**, *23*, 1514−1521.

(16) Ye, H.; Cande, C.; Stephanou, N. C.; Jiang, S.; Gurbuxani, S.; Larochette, N.; Daugas, E.; Garrido, C.; Kroemer, G.; Wu, H. DNA Binding is Required for the Apoptogenic Action of Apoptosis Inducing Factor. *Nat. Struct. Biol.* **2002**, *9*, 680−684.

(17) Susin, S. A.; Lorenzo, H. K.; Zamzami, N.; Marzo, I.; Snow, B. E.; Brothers, G. M.; Mangion, J.; Jacotot, E.; Costantini, P.; Loeffler, M.; Larochette, N.; Goodlett, D. R.; Aebersold, R.; Siderovski, D. P.; Penninger, J. M.; Kroemer, G. Molecular Characterization of Mitochondrial Apoptosis-Inducing Factor. *Nature* **1999**, *397*, 441−446.

(18) Lassus, P.; Opitz-Araya, X.; Lazebnik, Y. Requirement for Caspase-2 in Stress-Induced Apoptosis Before Mitochondrial Permeabilization. *Science* **2002**, *297*, 1352−1354.

(19) Marsden, V. S.; O'Connor, L.; O'Reilly, L. A.; Silke, J.; Metcalf, D.; Ekert, P. G.; Huang, D. C.; Cecconi, F.; Kuida, K.; Tomaselli, K. J.; Roy, S.; Nicholson, D. W.; Vaux, D. L.; Bouillet, P.; Adams, J. M.; Strasser, A. Apoptosis Initiated by Bcl-2-Regulated Caspase Activation Independently of the Cytochrome *c*/Apaf-1/Caspase-9 Apoptosome. *Nature* **2002**, *419*, 634−637.

(20) Cory, S.; Huang, D. C.; Adams, J. M. The Bcl-2 Family: Roles in Cell Survival and Oncogenesis. *Oncogene* **2003**, *22*, 8590−8607.

(21) Green, D. R.; Kroemer, G. The Pathophysiology of Mitochondrial Cell Death. *Science* **2004**, *305*, 626−629.

Chemotherapeutic agents can induce apoptosis by affecting specific organelles including nuclei, mitochondria, the endoplasmic reticulum, or lysosomes. Because macromolecular therapeutics possess a different mechanism of cell entry and intracellular distribution than free drugs, a different mechanism for the induction of apoptosis was proposed. Differences in gene expression profiles and mechanism of action when comparing free drugs with drug delivery systems has been reported by several research groups. Nishiyama et al.[23] observed differences in the gene expression profiles of non-small cell lung cancer PC-14 cells exposed to free cisplatin and cisplatin incorporated into polymeric micelles. Kabanov et al.[24] have found a significant change in the genomic responses of human breast carcinoma MCF7 cells when doxorubicin was combined with Pluronic, an amphiphilic triblock copolymer of poly(ethylene oxide) and poly(propylene oxide). Compared with free drug, treatment of cells with doxorubicin formulated with Pluronic block copolymer P85 significantly promoted apoptotic cell death by increasing the expression of genes of pro-apoptotic proteins and downregulating the expression of genes of anti-apoptotic proteins.[25] Differences in gene expression profiles of drug-sensitive (A2780) and doxorubicin-resistant (A2780/AD) human ovarian carcinoma cells were detected after exposure to free and HPMA copolymer-bound doxorubicin in vitro[26] and in vivo[27] (Figure 1). It has been demonstrated that HPMA copolymer-bound doxorubicin can overcome MDR1 gene-encoded resistance,[28] and activate apoptosis in human ovarian cancer cells by the Fas-independent pathway.[29] Říhová and colleagues noted differences in the intracellular distribution of free and polymer-bound doxorubicin in several types of tumor cells[30] and their different effects on the expression of genes involved in the regulation of cell cycle and apoptosis,[31] and suggested that HPMA copolymer-bound doxorubicin induced apoptosis in tumor cells by affecting mitochondria. However, no studies on the effects of macromolecular therapeutics on protein levels were reported. The present study elucidated the effects of HPMA copolymer-bound doxorubicin on the induction of the mitochondrial pathway of programmed cell death and the involvement of the Bcl-2 family proteins in this process.

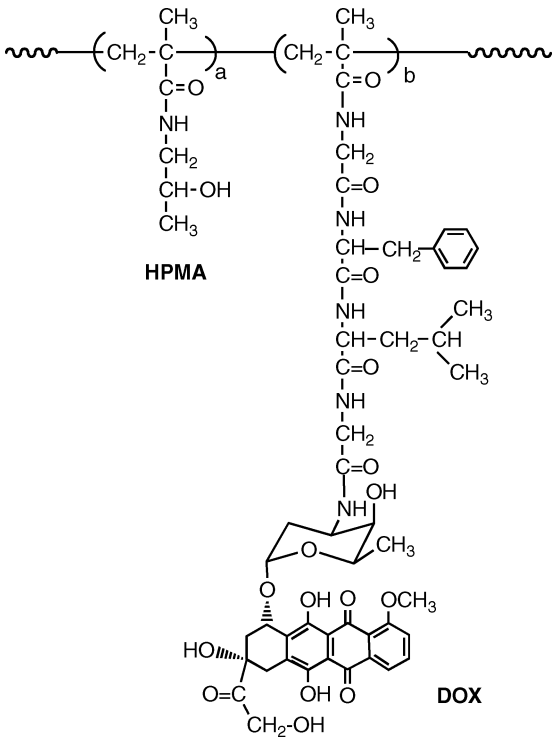

Figure 1. Structure of HPMA copolymer−doxorubicin conjugate (P-GFLG-DOX). P is the HPMA copolymer backbone; GFLG (Gly-Phe-Leu-Gly) is a lysosomally degradable spacer. The conjugate contained 0.11 mmol of doxorubicin/g of polymer (6.4 wt %); molecular weight, $M_w = 27$ kDa.

Experimental Methods

Chemicals. DOX was a kind gift from Dr. A. Suarato, Pfizer, Milano, Italy. Stock solutions (3 mM) were prepared in distilled water, filtered through a 0.2 μm membrane,

(22) Huang, Z. Bcl-2 Family Proteins as Targets for Anticancer Drug Design. *Oncogene* **2000**, *19*, 6627−6631.

(23) Nishiyama, N.; Koizumu, F.; Okazaki, S.; Matsumura, Y.; Nishio, K.; Kataoka, K. Differential Gene Expression Profile Between PC-14 Cells Treated with Free Cisplatin and Cisplatin-Incorporated Polymeric Micelles. *Bioconjugate Chem.* **2003**, *14*, 449−457.

(24) Kabanov, A. V.; Batrakova, E. V.; Sriadibhatla, S.; Yang, Z.; Kelly, D. L.; Alakhov, V. Yu. Polymer Genomics: Shifting the Gene and Drug Delivery Paradigms. *J. Controlled Release* **2005**, *101*, 259−271.

(25) Minko, T.; Batrakova, E. V.; Li, S.; Li, Y.; Pakunlu, R. I.; Alakhov, V. Yu.; Kabanov, A. V. Pluronic Block Copolymers Alter Apoptotic Signal Transduction of Doxorubicin in Drug-Resistant Cancer Cells. *J. Controlled Release* **2005**, *105*, 269−278.

(26) Minko, T.; Kopečková, P.; Kopeček, J. Comparison of the Anticancer Effect of Free and HPMA Copolymer-Bound Adriamycin in Human Ovarian Carcinoma Cells. *Pharm. Res.* **1999**, *16*, 986−996.

(27) Minko, T.; Kopečková, P.; Kopeček, J. Efficacy of Chemotherapeutic Action of HPMA Copolymer-Bound Doxorubicin in a Solid Tumor Model of Ovarian Carcinoma. *Int. J. Cancer* **2000**, *86*, 108−117.

(28) Minko, T.; Kopečková, P.; Pozharov, V.; Kopeček, J. HPMA Copolymer-Bound Adriamycin Overcomes MDR1 Gene Encoded Resistance in a Human Ovarian Carcinoma Cell Line. *J. Controlled Release* **1998**, *54*, 223−233.

(29) Malugin, A.; Kopečková, P.; Kopeček, J. HPMA Copolymer-Bound Doxorubicin Induces Apoptosis in Human Ovarian Carcinoma Cells by a Fas-Independent Pathway. *Mol. Pharm.* **2004**, *1*, 174−182.

(30) Hovorka, O.; Šťastný, M.; Etrych, T.; Šubr, V.; Strohalm, J.; Ulbrich, K.; Říhová, B. Differences in the Intracellular Fate of Free and Polymer-Bound Doxorubicin. *J. Controlled Release* **2002**, *80*, 101−117.

(31) Kovář, M.; Kovář, L.; Šubr, V.; Etrych, T.; Ulbrich, K.; Mrkvan, T.; Loučka, J.; Říhová, B. HPMA Copolymers Containing Doxorubicin Bound by a Proteolytically or Hydrolytically Cleavable Bond: Comparison of Biological Properties In Vitro. *J. Controlled Release* **2004**, *99*, 301−314.

aliquoted, and stored at −20 °C. P-GFLG-DOX (Figure 1; P is the HPMA copolymer backbone; GFLG (Gly-Phe-Leu-Gly) is a lysosomally degradable spacer) was synthesized as previously described.[32] The conjugate was extensively purified from the free drug by chromatography using a Sephadex LH-20 column (5 × 60 cm) in methanol + 0.2% acetic acid (three consecutive runs of 0.5 g of conjugate). The conjugate contained 0.11 mmol of DOX/g of polymer (6.4 wt %); molecular weight, $M_w = 27$ kDa; polydispersity, $M_w/M_n = 1.4$. P-GFLG-DOX stock solutions (6 mM) were prepared in distilled water, filtered through a 0.2 μm membrane, aliquoted, and stored at −20 °C. All concentrations of P-GFLG-DOX were expressed in DOX equivalents. 5,5′,6,6′-Tetrachloro-1,1′,3,3′-tetraethylbenzimidazolylcarbocyanine iodide (JC-1) was purchased from Cell Technology Inc. (Minneapolis, MN). Bovine serum albumin (BSA), Igepal CA 630, bovine pancreatic RNase A, protease inhibitors, phosphate-buffered saline (PBS), and RPMI-1640 medium were purchased from Sigma Chemical Co. (St. Louis, MO). All reagents for SDS−PAGE and Western blotting were purchased from Bio-Rad Laboratories (Hercules, CA). Fetal bovine serum (FBS), 0.05% trypsin, and 0.02% EDTA (trypsin−EDTA) solution were purchased from HyClone Laboratories (Ogden, UT).

Determination of the Amount of Free DOX in the Conjugate. Two milligrams of P-GFLG-DOX was applied to the Superdex Peptide HR 10/30 column in the FPLC/AKTA system Pharmacia, using 0.1 M sodium acetate pH 5.5 buffer containing 30 vol % acetonitrile (UV detection). Using a flow rate of 0.5 mL/min, the polymer peak was eluted at the exclusion limit of the column (20−25 min), and the fraction corresponding to the free DOX was collected at the interval of 36.5−38.5 min (based on the calibration using free DOX). The concentration of free DOX in the fraction collected from the column was measured by fluorescence spectroscopy using fluorescence spectrophotometer LS-55 (emission spectra scanned in the range 510−700 nm, exc 488 nm, in a 1 cm cuvette). A DOX calibration curve was used for the calculation of the free drug concentration. The content of free DOX was 0.14% relative to the bound drug. This method ensures that only low-molecular weight DOX is detected and that it is sensitive in the nanomole/liter concentration range.

Antibodies. Primary antibodies used in immunoblot analysis were as follows: mouse monoclonal anti-human Bad (1:1000); rabbit Bax polyclonal antibody (1:1000); mouse monoclonal anti-human Bcl-2 (1:1000); rabbit polyclonal anti-human BCL-x_L (1:400); mouse anti-human AIF (1:1000) from Santa Cruz Biotechnology Inc., Santa Cruz, CA); rabbit polyclonal anti-human Bid (1:400; Biosource, Camarillo, CA); mouse monoclonal anti-human COX-IV (1:1000, Mitosciences, Eugene, OR); and anti-human actin antibody from Oncogene Research Products (San Diego, CA). Secondary antibodies were donkey anti-goat (1:5000), bovine anti-goat (1:5000) from Santa Cruz Biotechnology Inc., goat anti-rabbit (1:8000) or goat anti-mouse (1:10000) from Southern Biotechnology Ass. Inc. (Birmingham, AL) antibodies conjugated to horseradish peroxidase, as appropriate.

Cells. The A2780 cell line, a human ovarian carcinoma was obtained from T. C. Hamilton (Fox Chase Cancer Center, Philadelphia, PA). Cells were grown in RPMI 1640 media supplemented with 10% FBS, 2 mM glutamine at 37 °C in 5% CO_2 and 95% humidified air. The cells were regularly subcultured to maintain them in a logarithmic phase of growth. Cells were plated into appropriate plastic ware with an initial density 3×10^4 cells/cm^2. Experiments were initiated 48 h after plating of cells, unless otherwise stated. Cells were detached by applying trypsin−EDTA for 1 min and were processed for flow cytometry or Western blot analysis as described below.

Cell Viability. Drug cytotoxicity toward A2780 cells was evaluated as described previously.[29] The IC_{50} doses found were 0.05 ± 0.01 and 7.2 ± 2.5 μM for free DOX and P-GFLG-DOX, respectively (continuous drug exposure for 72 h[29]). In this study, the induction of apoptosis was assessed at a doses 2 × $IC_{50,}$ if not otherwise stated. Cell survival also was evaluated in parallel with JC-1 time course experiments. A2780 cells were plated into 6-well plates and after 48 h incubation were treated with both forms of doxorubicin at the indicated time intervals. Viable cells were determined by trypan blue dye exclusion and were enumerated in a Neubauer hemocytometer. Cell counts were performed in duplicate for each drug dose and time point, with SEM typically lower than 15%.

Subcellular Fractionation. Control or treated cells (5×10^7) were washed twice with cold phosphate-buffered saline (PBS), collected, and resuspended in an isotonic buffer containing 20 mM Hepes, pH 7.5, 250 mM sucrose, 10 mM KCl, 1.5 mM $MgCl_2$, 1 mM EGTA, 1 mM EDTA, and a mixture of protease inhibitors (Sigma). After 30 min on ice, the cells were homogenized for 30 strokes with a dounce homogenizer. In preliminary experiments, it was confirmed that the treatment was sufficient to disrupt 70−80% of cells. The homogenate was then centrifuged (750 g for 10 min) to pellet unlysed cells and nuclei. Supernatants were collected and centrifuged at 10000*g* for 30 min to pellet the mitochondria-rich heavy membrane fraction. The supernatant (cytosolic fraction) was removed, and the heavy membrane pellet (mitochondrial fraction) was suspended in lysis buffer supplemented with 1% Triton X-100. After determination of protein content, the fractions were used for an immunoblotting analysis for cytochrome *c* or AIF. The detection of the mitochondrial protein COX subunit IV was used to confirm that no cross-contamination of cytosolic fraction by the fractionation method occurred.

Immunoblotting. A2780 cells were incubated for 24 h with both forms of DOX. The cells were then rinsed once with PBS and solubilized with buffer containing 25 mM Tris·

(32) Omelyanenko, V. G.; Kopečková, P.; Gentry, C.; Shiah, J.-G.; Kopeček, J. HPMA Copolymer-Anticancer Drug-OV-TL16 Antibody Conjugates. 1. Influence of the Methods of Synthesis on Binding Affinity to OVCAR-3 Ovarian Carcinoma In Vitro. *J. Drug Targeting* **1996**, *3*, 357−373.

HCl, 250 mM sodium chloride, 2 mM EDTA, 1% Triton X-100, 1 mM PMSF, and a mixture of protease inhibitors (Sigma). The cell lysates were centrifuged at 10000*g* for 15 min to remove debris. The protein concentration in each supernatant was determined using the Coomassie Plus Protein Assay (Pierce, Rockford, IL), and equal amounts of protein (50 μg/lane) were separated by 15% SDS−PAGE. The resolved proteins were electroblotted onto a nitrocellulose membrane in transfer buffer (192 mM glycine, 20% methanol, 25 mM Tris HCl). The transfer was confirmed by reversibly staining the membrane with Pounceau S solution. To reduce nonspecific binding, the membranes were incubated in a blocking buffer (20 mM Tris, pH 7.6, 137 mM sodium chloride, 2% BSA, 0.1% Tween-20) at 4 °C overnight. Membranes were then incubated with specific primary antibodies at the indicated dilution for 1 h at room temperature, and rinsed in washing buffer (Tris-buffered saline, pH 7.6, and 0.1% Tween-20) three times for 10 min each. Blots were probed with relevant primary antibody, followed by incubation with an appropriate secondary antibody conjugated with horseradish peroxidase. Chemiluminescent signals were generated by the addition of ECL reagent (Amersham Biosciences Corp., Piscataway, NJ). Quantification of protein bands was performed using Quantity One (version 4.3.1; Bio-Rad Laboratories) software. The relative amounts of each protein were normalized to the respective signals from β-actin.

Mitochondrial Membrane Potential. Three different methods were employed to detect mitochondrial membrane potential changes using the fluorescent probe JC-1. JC-1, a lipophilic cationic dye, easily passes through the plasma membrane into cells and accumulates in actively respiring mitochondria.[33] The degree of accumulation of JC-1 in mitochondria depends on the membrane potential. At a low mitochondrial membrane potential, there is very little accumulation of the dye; consequently, the dye exists as a monomer that emits green fluorescence. As the mitochondrial membrane potential increases, the accumulation of the dye in mitochondria increases too. At higher concentrations the dye forms "J-aggregates". Dye aggregation leads to a shift in the fluorescence emission from green to red. J-aggregate formation is a fast and reversible process, which occurs in specific regions with higher potential, and can be used as a sensitive tool for investigating the mitochondrial membrane potential changes.[34]

For flow cytometry, cells were treated for 24 h with drugs in 6-well plates and were then washed three times with warm PBS. The cells were then detached with trypsin−EDTA solution. Collected cells were incubated for 15 min with 1 μg/mL of JC-1 in culture medium at 37 °C in the dark. Stained cells were collected in warm PBS/2% BSA and washed twice by centrifugation. Finally, cells were resuspended in 0.3 mL of PBS with 2% BSA and used for acquisition. A FACScan (Becton Dickinson Biosciences, Mountain View, CA) equipped with a single 488 nm argon laser was used in our study. After the flow cytometer was set for green (FL-1) and red (FL-2) fluorescence, the data were collected and analyzed with Cell Quest software (BD Biosciences).

A PerkinElmer LS-55 spectrofluorometer equipped with plate reader (PerkinElmer Instruments, Norwalk, CT) was used to perform time course studies on the effects of DOX and P-GFLG-DOX on cellular JC-1 fluorescence. Adherent A2780 cells were treated with drugs or control medium in 24-well plates for the indicated time intervals and then washed two times with warm PBS/2% FBS. A prewarmed solution of JC-1 in growth media was added to wells to a final concentration of 2 μg/mL. After a 30 min incubation, the cells were washed twice with warm PBS, and fluorescence measurements were taken using 530 nm excitation (Ex)/590 nm emission (Em) for red J-aggregate fluorescence and 485 nm Ex/530 nm Em for green fluorescence. After subtraction of background, values obtained from wells containing cells without JC-1, red/green fluorescence ratios were calculated.

For fluorescence microscopy, cells were grown on 35 mm glass bottom microwell dishes (MatTek, Ashland, MA). Fresh staining solution (1 μg/mL) was prepared immediately before use by diluting a 100× stock solution of JC-1 in warm (37 °C) culture medium supplemented with 10% FBS. Cells treated with drugs, as above, were incubated with JC-1 for 30 min in a 37 °C CO_2 incubator. Cells were then washed twice with warm PBS and examined immediately under a laser scanning confocal microscope Olympus FluoView 1000 (Minneapolis, MN). The JC-1 was excited at 488 nm, and light emissions were collected between 515 and 545 nm (green) and at 570−600 nm (red). All image acquisitions and analyses were performed using FluoView software. The intensity of the laser beam and the photodetector sensitivity were kept constant in order to compare the relative fluorescence intensities between experiments.

Statistical Analysis. Data are expressed as mean ± SEM, where appropriate.

Results

The apoptotic changes in mitochondria can be observed either by detecting the release of mitochondrial proteins into the cytoplasm or by alterations of mitochondrial function. Because the mitochondrial membrane potential is a vital component of respiring mitochondria and is linked to many mitochondrial functions, its changes after drug treatment were observed by monitoring the intensity and shift of fluorescence emission of the JC-1 dye. The positively charged lipophilic JC-1 dye accumulates in the matrix of mitochondria because of negative potential of the inner mitochondrial membrane.[35] When a critical concentration is reached, JC-1 forms J-aggregates. Dye J-aggregates have a red fluorescence emission peak in contrast to the green fluorescence emission peak

(33) Reers, M.; Smith, T. W.; Chen, L. B. J-Aggregate Formation of a Carbocyanine as a Quantitative Fluorescent Indicator of Membrane Potential. *Biochemistry* **1991**, *30*, 4480−4486.

(34) Reers, M.; Smiley, S. T.; Mottola-Hartshorn, C.; Chen, A.; Lin, M.; Chen, L. B. Mitochondrial Membrane Potential Monitored by JC-1 Dye. *Methods Enzymol.* **1995**, *260*, 406−417.

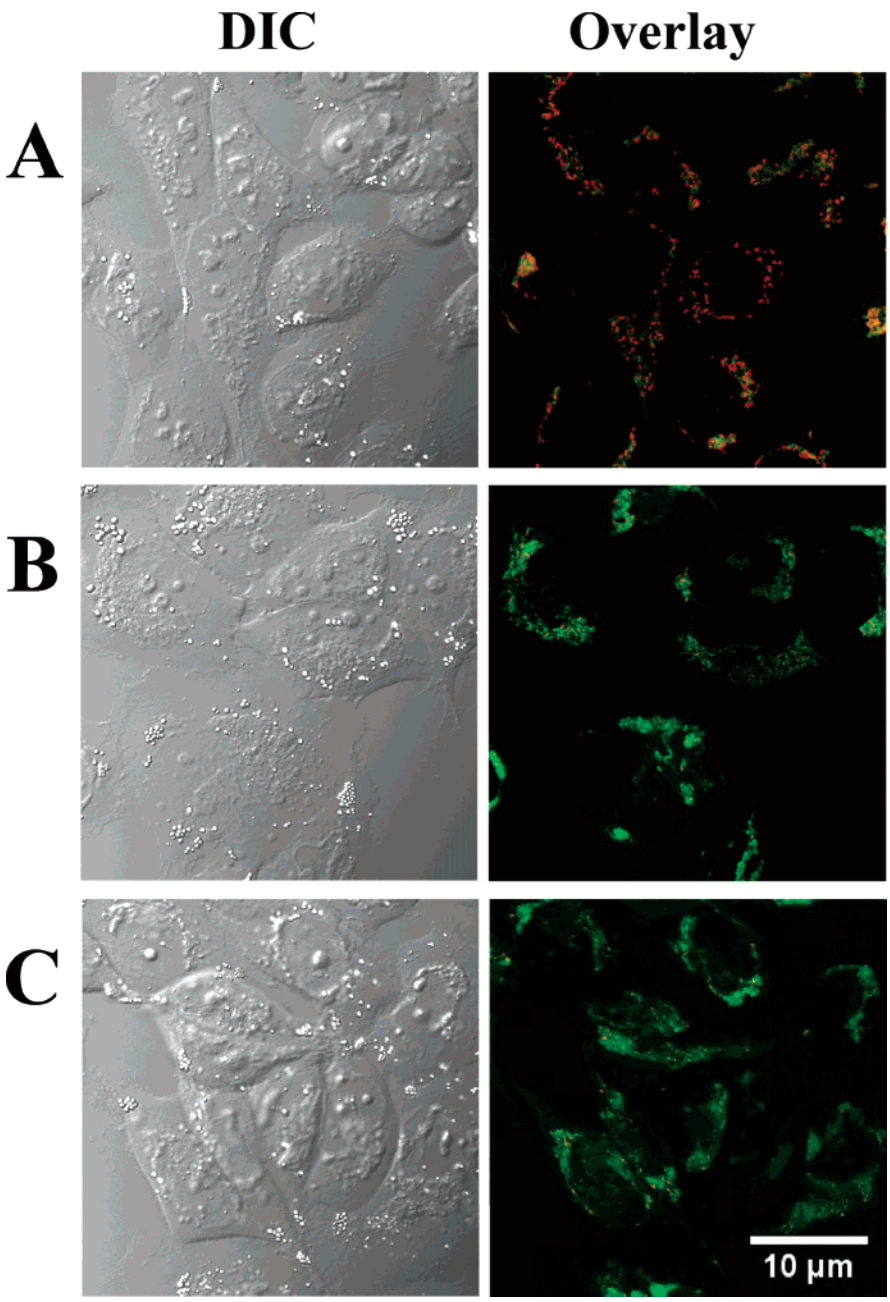

Figure 2. An alteration of JC-1 staining in A2780 cells. Cells were cultured in 35 mm dishes and exposed to 2 × IC_{50} DOX and P-GFLG-DOX for 24 h. After being incubated with drugs, cells were loaded with JC-1, washed, and analyzed under a laser scanning confocal microscope. Incubation of A2780 cells with free DOX or P-GFLG-DOX resulted in the collapse of mitochondrial potential. It is manifested with a decrease of red fluorescence (JC-1 aggregated form) and an increase of green fluorescence (JC-1 monomer form). (A) Control cells. (B) DOX treated cells. (C) P-GFLG-DOX treated cells. Scale bar = 10 μm.

of dye monomers. As shown by Chen's group, the existence of an electrochemical gradient is necessary for the formation and maintenance of the J-aggregates in mitochondria.[35] The destruction of the normal electrochemical gradient decreases the mitochondrial membrane potential causing the loss of red fluorescence as well as an increase of cytoplasmic green fluorescence. Figure 2 shows the changes of A2780 cell fluorescence as a result of drug treatment. Untreated A2780 cells loaded with JC-1 exhibited a heterogeneous distribution of green fluorescence (JC-1 monomers) and red fluorescence (JC-1 aggregates). Some cells showed both green and red-orange fluorescence (Figure 2). These modes of J-aggregate distribution, even in the same cell or the same mitochondria, possibly reflect the physiological modulation of mitochondrial activity in living cells.[35] Exposure of A2780 cells to

(35) Smiley, S. T.; Reers, M.; Mottola-Hartshorn, C.; Lin, M.; Chen, A.; Smith, T. W.; Steele, G. D., Jr.; Chen, L. B. Intracellular Heterogeneity in Mitochondrial Membrane Potentials Revealed by a J-Aggregate-Forming Lipophilic Cation JC-1. *Proc. Natl. Acad. Sci. U.S.A.* **1991**, *88*, 3671−3675.

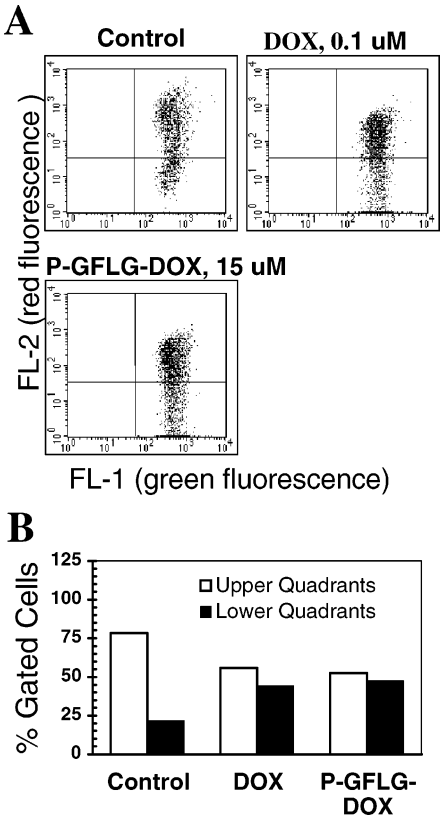

Figure 3. Flow cytometric analysis of A2780 cells loaded with JC-1 fluorescence dye. A2780 cells were treated with 2 × IC_{50} DOX or P-GFLG-DOX for 24 h. After trypsinization, the resulting cell suspension was stained with 1 μg/mL of JC-1 for 15 min at 37 °C, washed, and analyzed for green (FL-1) and red (FL-2) fluorescence by flow cytometry. (A) Dot-plot data generated using Cell Qwest software. (B) Distribution of gated cells in upper or lower quadrants as shown in panel A. Cells with altered mitochondrial membrane potential are located in the low right quadrant. The experiment was repeated at least three times with similar results.

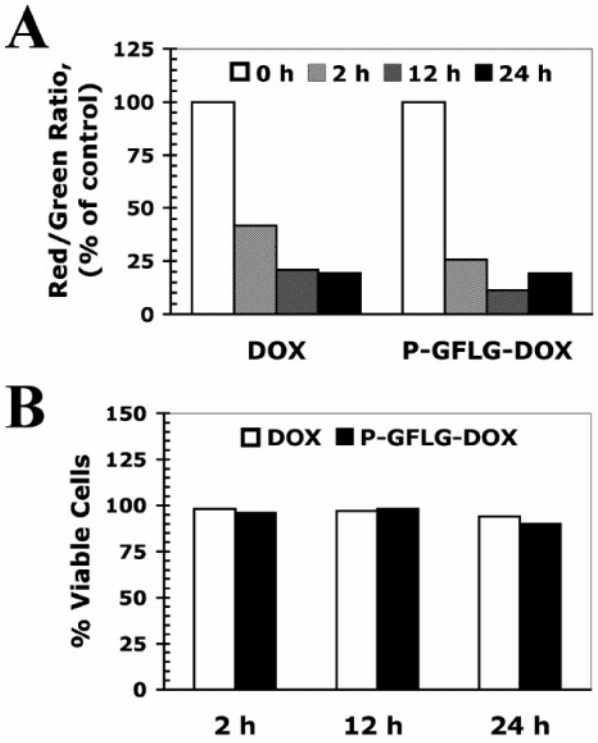

Figure 4. Time course measurement of the effects of DOX and P-GFLG-DOX on mitochondrial membrane potential using JC-1 dye. All assays were performed using a PerkinElmer LS55 spectrofluorometer equipped with a plate reader. Cells were incubated with 2 × IC_{50} DOX or P-GFLG-DOX for 24 h, washed, incubated with 1 μg/mL of JC-1 for an additional 30 min at 37 °C, washed again, and analyzed for the change of JC-1 fluorescence. JC-1 staining was performed using the kit purchased from Cell Technology, Inc. Data are shown as means of duplicate measurements of JC-1 fluorescence (A) or results of dye exclusion assays (B). The experiment was repeated twice with similar results.

both forms of doxorubicin resulted in changes in cell staining: the red-orange fluorescence regions decreased or disappeared, while green fluorescence intensity in the cytoplasm increased. It appeared that the increase of green fluorescence in the cytoplasm was more pronounced when cells were treated with P-GFLG-DOX. Observed changes in the cells' fluorescence suggest the decrease of dye aggregate accumulation in mitochondria and the diffusion of JC-1 molecules into cytosol following the increase in the permeability of the mitochondrial membrane with concomitant collapse of mitochondrial membrane potential.

Analysis of cells by flow cytometry revealed a decrease in red fluorescence detectable after treatment with P-GFLG-DOX (Figure 3A). The percentage of cells with red fluorescence decreased from 78% (control cells) to 53%, which corresponded with an increase of green fluorescence from 22% to 47% (Figure 3B). Free doxorubicin induced approximately the same degree of change in fluorescence. Both drugs were used at 2 × IC_{50} concentrations for 24 h. No further increase of cell population with green fluorescence was observed even when a 4 × IC_{50} concentration of both drugs was used (data not shown).

JC-1 fluorescence was also examined in living cells using a PerkinElmer spectrofluorometer equipped with a plate reader. Time course studies on the effect of HPMA copolymer-bound DOX revealed a rapid decrease in mitochondrial membrane potential, as determined from the ratio of red/green fluorescence (Figure 4A). Within the first 2 h of exposure to 0.05 μM DOX or 7.0 μM P-DOX, the red/green ratio declined to 45% or 26% of control, respectively. The most dramatic changes in mitochondrial membrane potential were observed between 2 and 12 h of continuous drug exposure. The mitochondrial membrane potentials remained collapsed when drug treatment continued up to 24 h. Monitoring of cell viabilities during time course experiments with the dye exclusion assay revealed no significant changes in the number of living cells during the first 24 h of continued drug exposure (Figure 4B). This data confirmed that mitochondrial function changes are the result of intracellular events, and do not depend on the integrity of the plasma membrane.

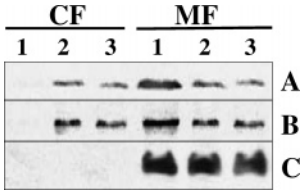

Figure 5. Release of cytochrome *c* (A) and AIF (B) from mitochondria into cytosol after exposure of A2780 cells to 2 × IC_{50} DOX or P-GFLG-DOX for 24 h. After treatment, A2780 cell lysates were fractionated and the cytosolic (CF) and the mitochondrial (MF) fractions were analyzed by Western blot using relevant primary antibodies. Blots were developed with ECL. Lane 1: Untreated cells. Lane 2: Cells treated with DOX. Lane 3: Cells treated with P-GFLG-DOX. (C) COX IV served as mitochondrial fraction marker.

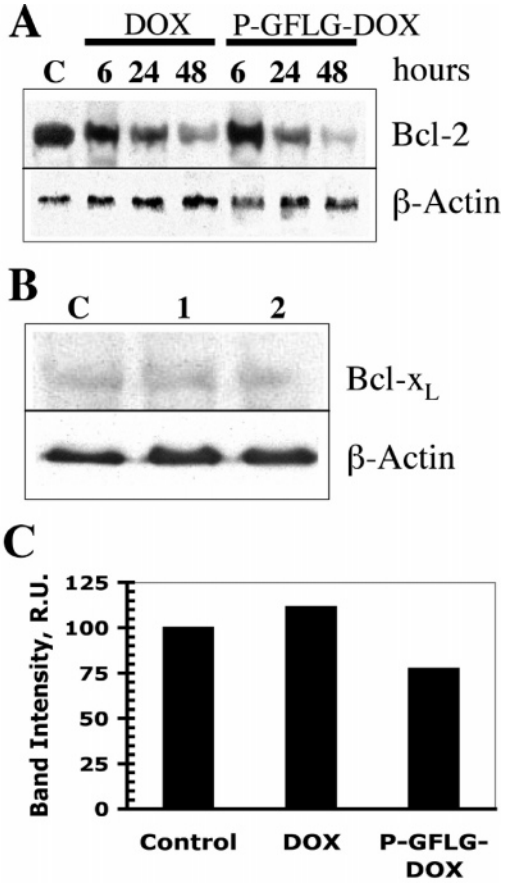

Figure 6. Expression regulation of anti-apoptotic proteins in A2780 cells treated with 2 × IC_{50} DOX and P-GFLG-DOX. Proteins (50 μg) from cell lysates were separated by 15% SDS−PAGE, transferred to membranes, and probed with relevant primary antibodies. Blots were developed with ECL. (A) Bcl-2 protein. (B) Bcl-x_L protein, 24 incubation with drugs. (C) Densitometry analysis of Bcl-x_L expression. Lane C: Untreated cells. Lane 1: DOX treated cells. Lane 2: P-GFLG-DOX treated cells. Data are representative of three independent experiments.

A decrease of mitochondrial membrane potential is often accompanied with an alteration of the mitochondrial membrane and the translocation of mitochondrial proteins to the cytosol. To check whether P-GFLG-DOX-induced mitochondrial potential collapse was accompanied by a translocation of mitochondrial proteins, the levels of cytochrome *c* in mitochondrial and the cytosolic fractions of A2780 cell lysates were assayed using Western blot analysis. The presence of cytochrome *c* was discovered in the cytosolic fraction of A2780 cells treated with both forms of doxorubicin, whereas no cytochrome *c* was found in the cytosolic fraction of untreated control cells (Figure 5). In addition, the release of AIF from mitochondria to the cytosol was detected when A2780 cells were treated with both forms of doxorubicin. The presence of other mitochondrial proteins, such as COX subunit IV, was not detected in the cytosolic fraction, confirming that an appropriate cell fractionation technique was used (Figure 5).

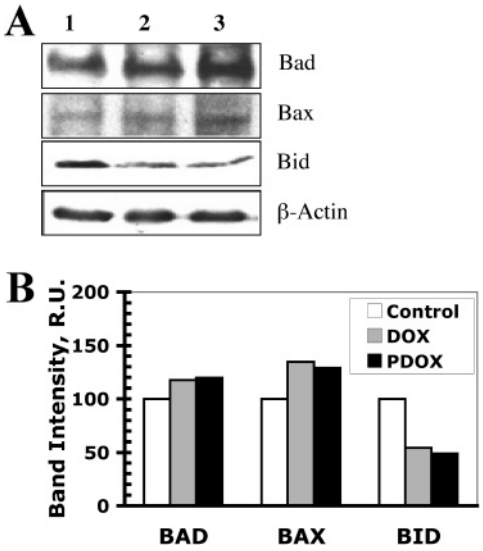

Figure 7. Expression regulation of pro-apoptotic proteins in A2780 cells treated with 2 × IC_{50} DOX and P-GFLG-DOX for 24 h. Proteins (50 μg) from cell lysates were separated by 15% SDS−PAGE, transferred to membranes, and probed with relevant primary antibodies. Blots were developed with ECL. (A) Typical Western blots images. Lane 1: Untreated cells. Lane 2: DOX treated cells. Lane 3: P-GFLG-DOX treated cells. Data are representative of three independent experiments. (B) Densitometry analysis of protein expression.

The maintenance of mitochondrial membrane integrity is highly dependent on the Bcl-2 family of proteins. These proteins play a critical role in the formation of mitochondrial membrane transition pores and the prevention of mitochondrial membrane potential loss.[22] A2780 cells were treated with both forms of doxorubicin for different period of times, followed by immunoblot analysis as described in Experimental Methods. It was found that the exposure of A2780 cells to both forms of doxorubicin resulted in a decreased expression of the anti-apoptotic proteins Bcl-2 and Bcl-x_L. It appeared that the most pronounced effect on Bcl-2 expression was observed when cells were treated with P-GFLG-DOX for 24 or 48 h (Figure 6A). Also, P-GFLG-DOX inhibited the expression of Bcl-x_L by 25% compared to control, whereas free DOX slightly stimulated the expres-

sion of Bcl-x_L by about 10% (Figure 6B,C). The expression levels of pro-apoptotic proteins, Bax and Bad, were slightly increased, but no significant differences in the effects of the two forms of DOX were observed (Figure 7A,B). It appeared that the expression of another pro-apoptotic protein (Bid) decreased significantly (Figure 7B). However, since the antibodies used were only capable of recognizing the full-size protein, the decreased amount of protein detected may only indicate truncation of Bid in the cytosol.

Discussion

Prior studies in our laboratory showed that incubation of human ovarian carcinoma A2780 cells with P-GFLG-DOX, as well as free DOX, resulted in the initiation of specific cellular events related to apoptosis. HPMA copolymer-bound doxorubicin-induced cell death was manifested by phosphatidylserine translocation in the plasma membrane,[29,36] activation of caspases on the gene[37] and protein[29] levels, and an increase in the number of Fas receptors on the plasma membrane.[29] However, it was found that the Fas receptor pathway was not decisive in the induction of apoptotic cell death in A2780 cells.[29] Since two major pathways of apoptosis are known, an investigation of involvement of the mitochondrial pathway in apoptosis induced by HPMA copolymer-bound doxorubicin was performed. The data presented in this study point to an important role for the mitochondrial pathway during P-GFLG-DOX-induced apoptosis.

Intensive studies over the past decade recognized mitochondria as the most important organelle involved in apoptosis initiation and regulation. To examine the functional activity of mitochondria, we monitored changes of the mitochondrial membrane potential with the fluorescent dye JC-1. The shift in the dye emission spectrum from red to green fluorescence was observed after treatment of cells with P-GFLG-DOX. Changes of the JC-1 dye fluorescence indicate the reduction of dye aggregate accumulation in mitochondria because of the decrease of mitochondrial membrane potential. Monitoring changes of the JC-1 dye fluorescence indicated that the collapse of the mitochondrial membrane potential induced by P-GFLG-DOX was a fast process. The ratio of red to green fluorescence dramatically decreased within the first 2−12 h and remained at a reduced level up to 24 h over the continuing observation. No significant changes in the permeability of plasma membrane were observed for the same period, confirming that impairment of mitochondrial function is not a consequence of apoptosis-associated damage to the plasma membrane.

A decrease of mitochondrial membrane potential is an indication of permeability transition pore opening. In eukaryotic cells, mitochondrial membrane permeabilization is an important event highlighting the "point of no return" in the death process.[38] Studies performed in the laboratory of Dr. Kroemer suggested that injuries to mitochondrial function are mediated by the permeability transition complex.[39,40] The permeabilization of the outer or inner mitochondrial membrane occurred upon induction of apoptosis by multiple cell death stimuli. In response to these stimuli, mitochondria can release several apoptogenic proteins that normally reside in the intermembrane space between the outer and inner mitochondrial membranes.[41]

To check whether mitochondrial membrane potential depletion accompanied increased mitochondria membrane permeabilization and mitochondrial proteins release, the presence of cytochrome *c* and AIF was examined in cytosol. Western blot analysis revealed the presence of cytochrome *c* in the cytosolic fraction of A2780 cell treated with P-GFLG-DOX (Figure 5). It is known that cytochrome *c*, upon release into the cytoplasm, promotes formation of the apoptosome, a multimeric Apaf-1/cytochrome *c* complex,[42] and triggers the activation of the caspase cascade.[43] Caspase activation ends with the activation of CAD, following CAD translocation to the nucleus and oligonucleosomal DNA fragmentation.[44] Moreover, it was reported recently that mitochondria can release other apoptogenic proteins such as Smac/Diablo and HtrA2/Omi.[45−47] These proteins also facilitate their apoptogenic potential through caspase activa-

(36) Demoy, M.; Minko, T.; Kopečková, P.; Kopeček, J. Time- and Concentration-Dependent Apoptosis and Necrosis Induced by Free and HPMA Copolymer-Bound Doxorubicin in Human Ovarian Carcinoma Cells. *J. Controlled Release* **2000**, *69*, 185−196.

(37) Minko, T.; Kopečková, P.; Kopeček, J. Preliminary Evaluation of Caspases-Dependent Apoptosis Signaling Pathways of Free and HPMA Copolymer-Bound Doxorubicin in Human Ovarian Carcinoma Cells. *J. Controlled Release* **2001**, *71*, 227−237.

(38) Penniger, J. M.; Kroemer, G.; Mitochondria, AIF and Caspases—Rivaling for Cell Death Execution. *Nat. Cell Biol.* **2003**, *5*, 97−99.

(39) Zamzami, N.; Marchetti, P.; Castedo, M.; Zanin, C.; Vayssiere, J. L.; Petit, P. X.; Kroemer, G. Reduction in Mitochondrial Potential Constitutes an Early Irreversible Step of Programmed Lymphocyte Death In Vivo. *J. Exp. Med.* **1995**, *181*, 1661−1672.

(40) Kroemer, G. The Mitochondrial Permeability Transition Pore Complex as a Pharmacological Target. An Introduction. *Curr. Med. Chem.* **2003**, *10*, 1469−1472.

(41) Wang, X. The Expanding Role of Mitochondria in Apoptosis. *Genes Dev.* **2001**, *15*, 2922−2933.

(42) Zou, H.; Li, Y.; Liu, X.; Wang, X. An APAF-1 Cytochrome *c* Multimeric Complex is a Functional Apoptosome that Activates Procaspase-9. *J. Biol. Chem.* **1999**, *274*, 11549−11556.

(43) Li, P.; Nijhawan, D.; Budihardjo, I.; Srinivasula, S. M.; Ahmad, M.; Alnemri, E. S.; Wang, X. Cytochrome *c* and dATP-Dependent Formation of Apaf-1/Caspase-9 Complex Initiates an Apoptotic Protease Cascade. *Cell* **1997**, *91*, 479−489.

(44) Sakahira, H.; Enari, M.; Nagata, S. Cleavage of CAD Inhibitor in CAD Activation and DNA Degradation During Apoptosis. *Nature* **1998**, *391*, 96−99.

(45) Du, C.; Fang, M.; Li, Y.; Li, L.; Wang, X. Smac, a Mitochondrial Protein that Promotes Cytochrome *c*-Dependent Caspase Activation by Eliminating IAP Inhibition. *Cell* **2000**, *102*, 33−42.

(46) Verhagen, A. M.; Ekert, P. G.; Pakusch, M.; Silke, J.; Connolly, L. M.; Reid, G. E.; Moritz, R. L.; Simpson, R. J.; Vaux, D. L. Identification of DIABLO, a Mammalian Protein that Promotes Apoptosis by Binding to and Antagonizing IAP Proteins. *Cell* **2000**, *102*, 43−53.

tion.[48,49] The data presented here are consistent with our previous observation that HPMA copolymer-bound doxorubicin induced activation of caspase 3 and caspase 9 in A2780 cells.[29]

Moreover, another protein usually located in the intermembrane space of mitochondria, AIF, was found in the cytosolic fraction of A2780 cells treated with P-GFLG-DOX (Figure 5). In response to apoptotic stimuli and increased outer mitochondrial membrane permeability, AIF, a 57 kDa flavoprotein, translocates to the nucleus, binds to DNA, and induces DNA fragmentation with the formation of large 50 kb fragments.[13,17,50] It is important to note that AIF does not cleave DNA by itself[49] but, rather, engages a nuclear endonuclease to perform DNA fragmentation and chromatin condensation, the hallmark events of apoptotic cell death.[16] It is interesting that even AIF-induced DNA fragmentation is caspase-independent; caspase activity is necessary for AIF escape from mitochondria to the cytosol.[51,52] Similar to AIF, endonuclease G translocation from the mitochondria to the nucleus resulted in DNA fragmentation independent of caspases.[50] The finding that P-GFLG-DOX could induce the release of AIF from mitochondria and initiate caspase-independent apoptosis supports our previous observation[29] that programmed cell death in A2780 cells probably takes place in the "type II" mode.[53]

These data suggest that caspase activation is not the only pathway of apoptotic cell death induction by P-GFLG-DOX. Other cellular events following drug treatment are able to induce cell death even in the absence of caspase activation. Release of cytochrome *c* can potentially block electron transfer and increase the production of reactive oxygen species with subsequent lipid peroxidation.[54,55] In our previous studies, it was found that P-GFLG-DOX was more effective than free doxorubicin in altering mitochondrial metabolism, inducing lipid peroxidation, and reducing cellular DNA content.[26,56] All these changes are closely related to the depletion of mitochondrial membrane potential, increased permeability transition, and the release and translocation of apoptogenic proteins to the nucleus.

The integrity of the mitochondrial outer membrane, mitochondrial permeability, and the release of mitochondrial proteins to the cytosol highly depend on the activity of members of the Bcl-2 protein family.[19−21] The involvement of this group of proteins in apoptotic processes has been intensively studied for the past decade; nevertheless, the precise molecular mechanism of the regulation of mitochondrial homeostasis by Bcl-2 family proteins remains unknown.[57] However, it is clear that the commitment of cells to die partially depends on the balance between pro-apoptotic proteins, such as Bad and Bax, and anti-apoptotic proteins that promote cell viability, such as Bcl-2 and Bcl-x_L.[19−21]

Because it was shown that P-GFLG-DOX causes mitochondrial dysfunction and release of mitochondrial proteins to the cytosol, we evaluated whether HPMA copolymer-bound doxorubicin affects the expression of the Bcl-2 family of proteins in A2780 cells. P-GFLG-DOX downregulated the expression of Bcl-2 in a time-dependent manner and also decreased the expression of Bcl-x_L. These findings correlate well with our previous observation that P-GFLG-DOX could downregulate the expression of Bcl-2 in A2780 cells on the gene level.[37] Concurrently, P-GFLG-DOX increased the expression of pro-apoptotic proteins Bax and Bad (Figure 7). It appeared that P-GFLG-DOX could affect the ratio of pro-apoptotic to anti-apoptotic proteins of the Bcl-2 family, critical for a cell's decision to die or not to die. The expression level of another pro-apoptotic protein Bid was lower than in the control, when cells were treated with both forms of DOX. This might indicate a possible cleavage of Bid in the cytosol and the formation of truncated tBid, which interacts with anti-apoptotic proteins in the outer mitochondrial membrane and initiates apoptosis.

In spite of intensive studies, the mechanism for cell cytotoxicity of P-GFLG-DOX has not been completely understood, and the results may sometimes appear contentious. The lack of a consensus theory for the mechanism of

(47) Suzuki, Y.; Imai, Y.; Nakayama, H.; Takahashi, K.; Takio, K.; Takahashi, R. A Serine Protease, HtrA2, is Released from the Mitochondria and Interacts with XIAP, Inducing Cell Death. *Mol. Cell*. **2001**, *8*, 613−621.

(48) Liu, Z.; Sun, C.; Olejniczak, E. T.; Meadows, R. P.; Betz, S. F.; Oost, T.; Herrmann, J.; Wu, J. C.; Fesik, S. W. Structural Basis for Binding of Smac/DIABLO to the XIAP BIR3 Domain. *Nature* **2000**, *408*, 1004−1008.

(49) Martins, L. M.; Iaccarino, I.; Tenev, T.; Gschmeissner, S.; Totty, N. F.; Lemoine, N. R.; Savopoulos, J.; Gray, C. W.; Creasy, C. L.; Dingwall, C.; Downward, J. The Serine Protease Omi/HtrA2 Regulates Apoptosis by Binding XIAP Through a Reaper-Like Motif. *J. Biol. Chem.* **2002**, *277*, 439−444.

(50) Li, L. Y.; Luo, X.; Wang, X. Endonuclease G is an Apoptotic DNase when Released from Mitochondria. *Nature* **2001**, *412*, 95−99.

(51) Yu, S. W.; Wang, H.; Poitras, M. F.; Coombs, C.; Bowers, W. J.; Federoff, H. J.; Poirier, G. G.; Dawson, T. M.; Dawson, V. L. Mediation of Poly(ADP-ribose) Polymerase-1-Dependent Cell Death by Apoptosis-Inducing Factor. *Science* **2002**, *297*, 259−263.

(52) Cregan, S. P.; Dawson, V. L.; Slack, R. S. Role of AIF in Caspase-Dependent and Caspase-Independent Cell Death. *Oncogene* **2004**, *23*, 2785−2796.

(53) Fulda, S.; Meyer, E.; Friesen, C.; Susin, S. A.; Kroemer, G.; Debatin, K. M. Cell Type Specific Involvement of Death Receptor and Mitochondrial Pathways in Drug-Induced Apoptosis. *Oncogene* **2001**, *20*, 1063−1075.

(54) Hockenbery, D. M.; Oltvai, Z. N.; Yin, X. M.; Milliman, C. L.; Korsmeyer, S. J. Bcl-2 Functions in an Antioxidant Pathway to Prevent Apoptosis. *Cell* **1993**, *75*, 241−251.

(55) Cai, J.; Wallace, D. C.; Zhivotovsky, B.; Jones, D. P. Separation of Cytochrome *c*-Dependent Caspase Activation from Thiol-Disulfide Redox Change in Cells Lacking Mitochondrial DNA. *Free Radical Biol. Med.* **2000**, *29*, 334−342.

(56) Minko, T.; Kopečková, P.; Kopeček, J. Chronic Exposure to HPMA Copolymer-Bound Adriamycin does Not Induce Multidrug Resistance in a Human Ovarian Carcinoma Cell Line. *J. Controlled Release* **1999**, *59*, 133−148.

(57) Tsujimoto, Y. Cell Death Regulation by the Bcl-2 Protein Family in the Mitochondria. *J. Cell Physiol.* **2003**, *195*, 158−167.

action of the free form of DOX, and insufficient knowledge about the intracellular fate and molecular targets of polymer-bound DOX, are among the reasons for the apparent discrepancies.

Free DOX may closely associate with the plasma membrane. In fact, plasma membrane has been suggested as the "most sensitive drug target" for DOX.[58] However, this interaction is not relevant to P-GFLG-DOX, since the drug is shielded by the hydrophilic polymer coil.[59] At the intracellular level, DOX could be responsible for multiple effects, including free radical formation, lipid peroxidation, inhibition of DNA topoisomerase II, DNA intercalation, DNA binding, alkylation, and cross-linking; inhibition of DNA replication, induction of DNA damage, cell growth arrest, and induction of cell differentiation and apoptosis [reviewed in ref 60]. The involvement of cytoplasmic components, especially mitochondria, in the apoptotic process induced by anthracyclines was also reported.[61] It was demonstrated that Bak activation resulted in cytochrome *c* release into the cytosol, followed by caspase cascade activation.[62] It was proposed that DOX induces mitochondrial malfunction through nonspecific oxidative damage of the outer and inner membranes, or through direct interaction with mitochondrial DNA, or by interacting with enzymes involved in cell respiration.[63] In addition, DOX may inhibit the activity of mitochondrial cytochrome oxidase (COX) by downregulating the expression of COX genes on both the mitochondrial and nuclear level.[64]

Upon internalization by endocytosis, the polymer-bound form of the drug can interact with intracellular molecular targets either in the endosomal/lysosomal compartment or, upon release of the free drug into the cytoplasm, with targets in the nucleus and other membrane-bound organelles.[59,65] The accumulation of DOX at or inside mitochondria is one likely scenario. Depending on the concentration reached, DOX could directly or indirectly block the respiration chain, inhibit enzymes, initiate an oxidative stress that would then damage mitochondrial membranes, or interact with the members of the Bcl-2 family. The data presented here has shown that P-GFLG-DOX induces apoptosis in A2780 cells by altering mitochondrial function, as indicated by the change of mitochondrial membrane potential, and release of cytochrome *c* and AIF into the cytoplasm. It is probable that the observed changes in mitochondrial function were mediated by the Bcl-2 family of proteins. However, the exact molecular target(s) and the sequence of events involved in cell death resulting from exposure to P-GFLG-DOX require further clarification.

Conclusions

Our results suggest that, during apoptosis induced by free doxorubicin and HPMA copolymer-bound doxorubicin, mitochondrial dysfunction occurs. This was determined to be mediated through mitochondrial events, associated with a decrease in mitochondrial membrane potential, cytochrome *c* and AIF release, and downregulation of anti-apoptotic proteins of the Bcl-2 family. Further work is needed to evaluate the differential involvement of the Bcl-2 family proteins and the exact sequence of events resulting in disruption of mitochondrial function during apoptosis induced by HPMA copolymer-bound doxorubicin.

Abbreviations

AIF, apoptosis-inducing factor; Bad, Bcl2-antagonist of cell death; Bcl-2, B-cell lymphoma/leukemia 2; Bid, Bcl-2 interacting domain; CAD, caspase-dependent DNase; DOX, doxorubicin; COX, cytochrome *c* oxidase; ECL, enhanced chemiluminescence; FBS, fetal bovine serum; GFLG, glycylphenylalanylleucylglycine; HPMA, *N*-(2-hydroxypropyl)-methacrylamide; MDR, multidrug resistance; HtrA2/OMI (high-temperature requirement protein A2); P-GFLG-DOX, HPMA copolymer-bound DOX via a GFLG spacer; P, HPMA copolymer backbone; PBS, phosphate-buffered saline; PMSF, phenylmethylsulfonyl fluoride; Smac/DIABLO (second mitochondria-derived activator of caspase/direct IAP-binding protein with low PI); TNF/NGF, tumor necrosis factor/nerve growth factor.

Acknowledgment. We thank Dr. A. Suarato (Pfizer, Milano, Italy) for the generous gift of DOX, Dr. A. Nori (University of Utah) for her help with the confocal microscopy, and Jon Callahan (University of Utah) for carefully revising this manuscript. The research was supported in part by NIH Grant CA51578 from the National Cancer Institute.

MP050065E

(58) Tritton, T. R.; Yee, G. The Anticancer Agent Adriamycin can be Actively Cytotoxic without Entering Cells. *Science* **1982**, *217*, 248−250.

(59) Nori, A.; Kopeček, J. Intracellular Targeting of Polymer-Bound Drugs for Cancer Chemotherapy. *Adv. Drug Delivery Rev.* **2005**, *57*, 609−636.

(60) Gewirtz, D. A. A Critical Evaluation of the Mechanisms of Action Proposed for the Antitumor Effects of the Anthracycline Antibiotics Adriamycin and Daunorubicin. *Biochem. Pharmacol.* **1999**, *57*, 727−734.

(61) Jung, K.; Reszka, R. Mitochondria as Subcellular Targets for Clinically Useful Anthracyclines. *Adv. Drug Delivery Rev.* **2001**, *49*, 87−105.

(62) Panaretakis, T.; Pokrovskaja, K.; Shoshan, M. C.; Grander, D. Activation of Bak, Bax, and BH3-Only Proteins in the Apoptotic Response to Doxorubicin. *J. Biol. Chem.* **2002**, *277*, 44317−44326.

(63) Serafino, A.; Sinibaldi-Vallebona, P.; Lazzarino, G.; Tavazzi, B.; Di Pierro, D.; Rasi, G.; Ravagnan, G. Modifications of Mitochondria in Human Tumor Cells During Anthracycline-Induced Apoptosis. *Anticancer Res.* **2000**, *20*, 3383−3394.

(64) Papadopoulou, L. C.; Tsiftsoglou, A. S. Effects of Hemin on Apoptosis, Suppression of Cytochrome *c* Oxidase Gene Expression, and Bone-Marrow Toxicity Induced by Doxorubicin (Adriamycin). *Biochem. Pharmacol.* **1996**, *52*, 713−722.

(65) Omelyanenko, V.; Kopečková, P.; Gentry, C.; Kopeček, J. Targetable HPMA Copolymer-Adriamycin Conjugates. Recognition, Internalization, and Subcellular Fate. *J. Controlled Release* **1998**, *53*, 25−37.